N. Rajesh Mathivanan* and Chandra Mouli

Modeling the low-velocity impact characteristics of woven glass epoxy composite laminates using artificial neural networks

Abstract: In this work, a new methodology based on artificial neural networks (ANN) has been developed to study the low-velocity impact characteristics of woven glass epoxy laminates of EP3 grade. To train and test the networks, multiple impact cases have been generated using statistical analysis of variance (ANOVA). Experimental tests were performed using an instrumented falling-weight impact-testing machine. Different impact velocities and impact energies on different thicknesses of laminates were considered as the input parameters of the ANN model. This model is a feed-forward back-propagation neural network. Using the input/output data of the experiments, the model was trained and tested. Further, the effects of the low-velocity impact response of the laminates at different energy levels were investigated by studying the cause-effect relationship among the influential factors using response surface methodology. The most significant parameter is determined from the other input variables through ANOVA.

Keywords: artificial neural network (ANN); computational modeling; fiber; impact behavior; laminates.

*Corresponding author: N. Rajesh Mathivanan, Department of Mechanical Engineering, PES Institute of Technology, Bangalore 560085, India, e-mail: rajesh_mathi@yahoo.com
Chandra Mouli: School of Computing Science and Engineering, Vellore Institute of Technology, Vellore 632 014, India

1 Introduction

The need for a material that has a high strength-to-weight and stiffness-to-weight ratio, good fatigue, and better corrosive properties has provoked structural engineers to focus on composite materials. Hence, there has been a growing interest to use composite materials in structural applications because of their outstanding properties when compared with conventional materials. Studies on the impact loading response of composite structures have shown that such loading can cause a substantial amount of damage, resulting in significant reductions in their strength and stiffness. A number of reviews on impact damages in composite structures are available [1–3] and detail the experimental investigations and analytical and numerical models developed. Matrix deformation and microcracking, interfacial debonding, lamina splitting, delamination, fiber breakage, and fiber pull-out are the possible modes of failure in composite laminates subjected to impact loading. Although fiber breakage is the ultimate failure mode, the damage would initiate in the form of matrix cracking propagation and lamina splitting and lead to delamination. Hence, it becomes highly important to predict or determine their response to impact loading. Some experimental studies on the behavior of laminates subjected to low-velocity impact are found in previousl published references [4–9].

The design of structures and components using newly developed composite materials usually requires extensive (and expensive) testing programs. Ideally, the designer should be able to accurately assess the performance of a new material or an existing material under untested conditions using a relatively small database of test results. For these situations, when it is difficult to find an accurate mathematical-based solution and the existing data are incomplete, noisy, or complex, the biologically motivated computing paradigm of artificial neural networks (ANNs) has emerged as a superior modeling tool [10]. Because of their massively parallel structure and their ability to learn by example, ANN can deal with non-linear modeling for which an accurate analytical solution is difficult to obtain. ANN has already been used in medical applications, image and speech recognition, classification, and control of dynamic systems, among others, but only recently have they been used in modeling the mechanical behavior of fiber-reinforced composite materials.

Chandrashekhara et al. [11] have studied the contact force for low-velocity impacts on laminated composite plates using impact-induced strain and neural networks. They have proved that the ANN approach in the estimation of contact force to be a promising alternative

to more traditional techniques. Bezerra et al. [12] used ANN for the prediction of shear mechanical behavior of laminates. Chakraborty [13] proposed optimum network architecture to predict the presence of embedded delaminations in laminates using natural frequencies as indicative parameters and ANN as a learning tool. Graham et al. [14] developed an ANN methodology to speed the damage detection process for the non-destructive evaluation of impact-damaged carbon fiber composites. Fernández-Fdz et al. [15] have predicted the ballistic behavior of carbon fiber reinforced polymers (CFRPs) against high-velocity impact of solids using ANN.

Response surface methodology (RSM) is a series of mathematical and statistical techniques used for modeling and analyzing problems and has the objective of optimizing the responses [16]. It is a sequential experimentation strategy for empirical model building and optimization. RSM is often applied in the characterization and optimization of processes. RSM can determine and represent cause-effect relationships among input control factors that influence the responses as a two- or three-dimensional hypersurface. Most of the work in RSM has been focused on the case where there is only one response of interest. In material characterization, however, it is quite common that several response variables are of interest. In this case, the determination of optimum conditions on the input variables would require simultaneous consideration of all the responses. This is called a multiresponse problem. To date, several approaches have been proposed for multiresponse optimization (MRO) including the desirability function approach [17] and loss function approach. MRO problems often involve incommensurate and conflicting criteria in multiple responses. A number of investigations using RSM are carried out to determine the significant factors affecting the response [18, 19].

It has been observed from earlier works that the application of ANN in modeling the mechanical behavior of fiber-reinforced composite laminates subjected to low-velocity impact loading is very inadequate. Hence, the present work aims at developing an ANN model for the prediction of retardation, penetration, and absorbed energy in woven glass epoxy laminates. The experimental results were used to train and test the ANN model. As a secondary objective, quantitative and statistical analyses were performed to evaluate the effect of the process parameters on the low-velocity impact behavior of the laminates. The model of response to the variables is obtained by applying regression analysis. Finally, an analysis of variance (ANOVA) was performed to check the adequacy of the mathematical models.

2 Experimental procedure

2.1 Fabrication of the laminates

The tested material was woven glass fiber epoxy matrix composite laminates of EP3 grade fabricated at ICP Pvt. Ltd. (Bangalore, India) in three different thicknesses, namely 2, 4, and 6 mm. The fiber reinforcement was kept constant for each batch of plates. Woven 'E'-glass fabric type C of IS:11273 was used. An epoxy matrix based on Lapox L-12 resin and K-5 hardener was selected for making composite panels. Identical woven fabric layers were selected depending on the thickness of the composite laminates and fabricated by the hand lay-up process. The composite panels were first cured at room temperature for 12 h under a pressure of 0.2 MPa using a hydraulic press. The postcuring was carried out at 120°C for 4 h and then cooled to room temperature. The composition of the laminate is the following:

– Fiber: E-glass plain weave roving fabric (63%)
– Fiber orientation: warp and weff at 90°
– Reinforcement: Epoxy resin – Lapox L-12 (27%)
– Binder: araldite LY 556 (5%)
– Hardener: K-5 grade (5%); diluent: DY 021.

2.2 Low-velocity impact testing

The low-velocity impact tests were conducted using instrumented impact tester, equipped with a cylindrical dart of 10 mm diameter. The falling-weight impact test equipment setup is shown in Figure 1. The dart material used was steel. A standard equipment is used to acquire, sample, collect, and store the signal from a piezoelectric load cell positioned at the other extremity of the calibrated cylindrical rod that constitutes the dart.

In accordance with ASTM D3029 standard [20], a batch of square, thin (150 mm side with varying thicknesses; 2, 4, and 6 mm) specimens were tested. The specimens were firmly clamped using specifically designed clamping apparatus that has a central rectangular slot of 100×100 mm. In this experimental work, the variation of impact parameters such as impact velocity and impact energy on the different thicknesses of the laminates was examined to record responses such as retardation, penetration, and absorbed energy at the maximum load of woven glass epoxy laminates in an impact event. Because the results were found to be highly reproducible, three specimens were used for each test condition.

Figure 1 Instrumented falling-weight impact test equipment.

3 Neural network approach

3.1 Artificial neural networks

An ANN is a massive parallel information processing system with certain performance characteristics similar to biological neural systems. ANNs are developed as generalizations of the mathematical models of the human brain. The information is processed at a simple element called neuron [21, 22]. Connections are made between neurons through links. Each link has a weight. The structure of an artificial neuron is given in Figure 2.

The ANN is characterized by its architecture, i.e., the way the neurons are connected to each other. The weights represent information being used by the network to solve a particular problem. Each neuron has an internal state called the activation state, which is a function of the inputs received. Some neurons will interface with the real world to receive the input, and some neurons provide outputs to the real world. The rest of the neurons are hidden, in the sense that they are not accessible to the real world but plays a major role in computation. Initially, all the weights are normalized and generated randomly. A typical ANN has three layers, namely, input layer, hidden layer, and output layer. There can be one or more
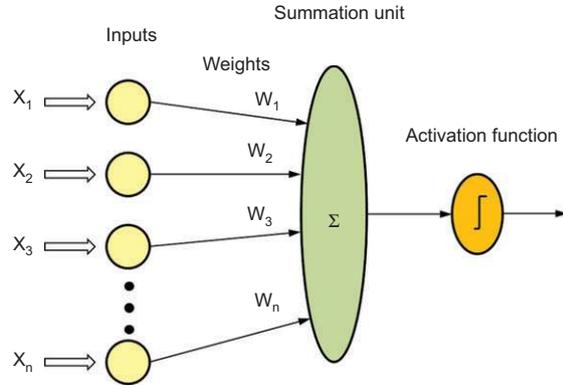

Figure 2 Structure of an artificial neuron.

hidden layers depending upon the number of dimensions of the training samples [23].

3.2 Data normalization

The data acquired are highly susceptible to noise, missing, and inconsistent due to the experimental setup. Data normalization is applied to improve the accuracy and efficiency of the behavioral characteristics of neural networks. By performing normalization, the data are scaled to a specific range, such as [0.0, 1.0] or [-1, 1]. The two standard measures for data normalization are min-max normalization and Z-score normalization [24, 25].

The min-max normalization performs a linear transformation on the original data. It preserves the relationships among the original values. For example, if $\min_A$ and $\max_A$ are the minimum and maximum values of an attribute A, the min-max normalization maps the value v of A to v' in the range [new_$\min_A$, new_$\max_A$] using the following Eq. (1)

$$v' = \frac{v - \min_A}{\max_A}(\text{new\_max}_A - \text{new\_min}_A) + \text{new\_min}_A \quad (1)$$

However, it will encounter the out-of-bounds error if a future input case for normalized data falls outside the original data range of A. In Z-score (or Z-mean normalization), the values of attribute A are normalized based on the mean and standard deviation of A. The value v of A is mapped to v' using Eq. (2), where std(A) gives the standard deviation of A.

$$v' = \frac{v - \text{mean}(A)}{\text{std}(A)} \quad (2)$$

With this normalization, the mean of the transformed values is reduced to zero. The Z-score normalization process is used to normalize the data.

3.3 Feed-forward neural network trained with back-propagation algorithm

The multilayered feed-forward neural network has been used in this article with one hidden layer of neurons. The feed-forward neural network is trained with training samples using the standard back-propagation algorithm. This training algorithm helps in determining the error obtained for the current training sample with the knowledge of the desired output. The error calculated is propagated back from output layer to the input layer through the hidden layers. At each hidden layer, as the back-propagated error is received; the weight adjustment factor is calculated and transmitted back to the input layer. At the input layer, the weights are adjusted based on the error, and again, the feed-forward training takes place. The overall training process consists of three stages: (a) feed-forward of the input pattern, (b) calculation and back-propagation of error, and (c) weight adjustment. The back-propagation algorithm used follows [26].

- Step 0: Initialize the weights. (The weights are set to small random values.)
- Step 1: When stopping condition are false, do steps 2–9.
- Step 2: For each training pair, do steps 3–8.

  Feed-forward:
- Step 3: Each input unit (X_i, $i=1...n$) receives input signal x_i and broadcasts this signal to all units in the layer above (to the hidden units).
- Step 4: Each hidden unit (Z_j, $j=1...p$) sums its weighted input signals,

$$z\_in_j = v_{oj} + \sum_{i=1}^{n} x_i v_{ij}, \tag{3}$$

applies its activation function to compare its output signal,

$$z_j = f(z\_in_j), \tag{4}$$

and sends the signal to all units in the layer above (to the output units).
- Step 5: Each output unit (Y_k, $k=1...m$) sums its weighted input signals,

$$y\_in_k = w_{ok} + \sum_{j=1}^{n} z_j w_{jk}, \tag{5}$$

and applies its activation function to compute its output signal.

$$y_k = f(y\_in_k). \tag{6}$$

Back-propagation of error:
- Step 6: Each output unit (Y_k, $k=1...m$) receives a target pattern corresponding to the input training pattern and computes its error information term,

$$\delta_k = (t_k - y_k) f'(y\_in_k), \tag{7}$$

calculates its weight correction term (used to update w_{jk} later),

$$\Delta w_{jk} = \alpha \delta_k z_j, \tag{8}$$

calculates its bias correction term (used to update w_{ok} later),

$$\Delta w_{ok} = \alpha \delta_k, \tag{9}$$

and sends δ_k to the units in the layer below.
- Step 7: Each hidden unit (Z_j, $j=1...p$) sums its δ inputs,

$$\delta\_in_j = \sum_{k=1}^{m} \delta_k w_{jk}, \tag{10}$$

is multiplied by the derivative of its activation function to calculate its error information term,

$$\delta_j = \delta\_in_j f'(z\_in_j), \tag{11}$$

calculates its weight correction term,

$$\Delta v_{ij} = \alpha \, \delta_j \, x_i, \tag{12}$$

and calculates its bias correction term,

$$\Delta v_{oj} = \alpha \, \delta_j. \tag{13}$$

Weight adjustment:
- Step 8: Each output unit (Y_k, $k=1...m$) updates its bias and weights ($j=0...p$):

$$w_{jk}(\text{new}) = w_{jk}(\text{old}) + \Delta w_{jk}. \tag{14}$$

Each hidden unit (Z_j, $j=1...p$) updates its bias and weights ($i=0...n$):

$$v_{ij}(\text{new}) = v_{ij}(\text{old}) + \Delta v_{ij}. \tag{15}$$

- Step 9: Test stopping condition.

3.4 Neural network design and training

Neural network learns the patterns by training with different types of sample data. Once the training is completed, the neural network is ready for generalization. The generalization capabilities of the neural network depends upon (a) the selection of the appropriate input/output parameters of the system, (b) the distribution of data set, and (c) the format of the presentation of the data set to the network. In this model, the three input parameters

used are laminate thickness, the impact velocity, and the impact energy. The three output parameters are retardation, penetration, and absorbed energy at maximum load. In this setup, the total number of experiments conducted were 325, of which two thirds of the data have been considered for training and one third of the data for testing. As mentioned, the input/output data sets are normalized before training using the Z-score normalization method. The standard multilayered feed-forward neural network trained with back-propagation algorithm is implemented in MATLAB 7.5 version. The network consists of one input layer with three neurons representing the three input parameters and one output layer with three output neurons indicating the three output parameters. The weights were randomly generated for the first iteration. The network was trained using the Levenberg-Marquardt algorithm. The network is trained initially with one neuron in the hidden layer, i.e., 3-1-3 topology was considered for training. In the subsequent phases, the number of hidden neurons in the hidden layer were increased gradually from 1 to 25 and then tested with two hidden layers with the same number of hidden neurons in the second hidden layer. The input/output data set of the model is illustrated schematically in Figure 3.

4 RSM and experimental design

As a secondary objective, experimental investigations were carried out on the design factors for low-velocity impact response. In RSM, it is possible to represent independent process parameters in quantitative form as
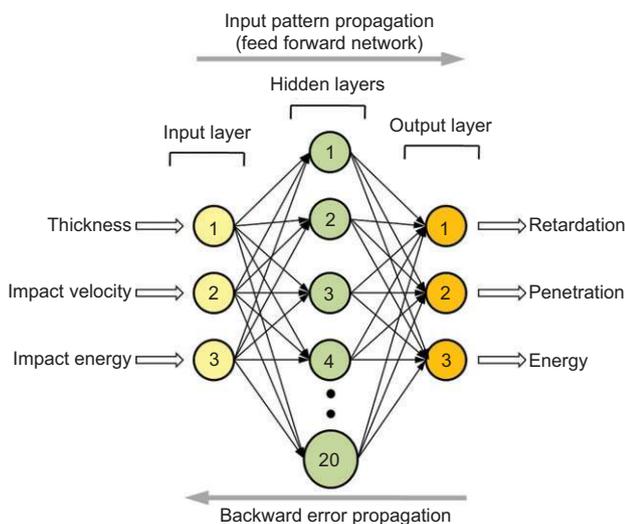
$$Y=f(X_1,X_2,X_3,\ldots\ldots X_n)\pm\varepsilon \qquad (16)$$

where Y is the response (yield), f is the response function, ε is the experimental error, and X_1, X_2, X_3...X_n are independent parameters. By plotting the expected response of Y, the response surface is obtained. The form of f is unknown and may be very complicated. Thus, RSM aims at approximating f by a suitable lower-ordered polynomial in some region of the independent process variables. If the response can be well modeled by a linear function of the independent variables, the function [Eq. (16)] can be written as

$$Y=C_0+C_1X_1+C_2X_2+\ldots+C_nX_n\pm\varepsilon \qquad (17)$$

However, if a curvature appears in the system, then a higher-order polynomial such as the quadratic model [Eq. (18)] may be used:

$$Y=C_0+\sum_{i=1}^{n}C_iX_n+\sum_{i=1}^{n}d_iX_i^2\pm\varepsilon \qquad (18)$$

The objective of using RSM is not only to investigate the response over the entire factor space but also to locate the region of interest where the response reaches its optimum or near-optimum value. By studying carefully the response surface model, the combination of factors that gives the best response can then be established.

The most imperative and influential of three significant factors, i.e., laminate thickness (A), impactor mass (B), and height of fall of the impactor (C), on the laminate subjected to low-velocity impact were studied. A face-centered central composite design was used to design the experiments for each parameter to predict the influence of each factor on the response. Each factor had two degrees of freedom. Hence, six was the summation of the total degrees of freedom of each factor. The levels for each impact testing parameters are shown in Table 1. The natural values in the levels for the height of fall and the impactor mass were selected based on the instrumented falling-weight impact test equipment boundaries, and the levels of the laminate thickness were selected based on the standard thickness commercially available.

To simplify the calculation, the natural values of input parameters are converted into coded values. The coded

Figure 3 Architecture of a multilayer perceptron: feed-forward network with backward propagation error (3-20-3).

Factors	Coding	Factor levels		
		-1	**0**	**1**
Thickness (mm)	X_1	2	4	6
Mass (N)	X_2	15.69	25.51	35.32
Height of fall (m)	X_3	0.5	1.0	1.5

Table 1 Parameters and their levels.

numbers for the variables used in tables are obtained from the following transformation equation:

$$X = \frac{X - X_{level\,0}}{X_{level\,+1} - X_{level\,0}} \tag{19}$$
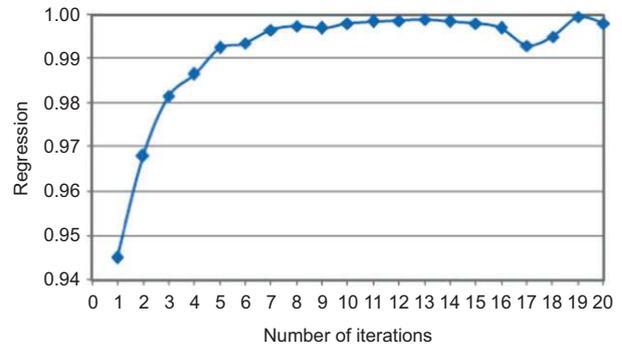
The Design Expert 8.0 software was used for the regression and graphical analyses of the data obtained. The optimum values of the selected variables were obtained by solving the regression equation and by analyzing the response surface contour plots. ANOVA was also performed to test the adequacy of the proposed models.

5 Results and discussion

The main objective of the present work was to study, predict, and analyze the low-velocity impact characteristics of glass epoxy composite laminates using back-propagation neural network (BPNN) and statistical analysis. The laminates of various thicknesses were subjected to low-velocity impact at energy levels ranging from 7.85 to 52.97 J. The effects of the process parameters, i.e., laminate thickness, impactor mass, and height of fall of the impactor, on the low-velocity impact behavior of the laminates were evaluated.
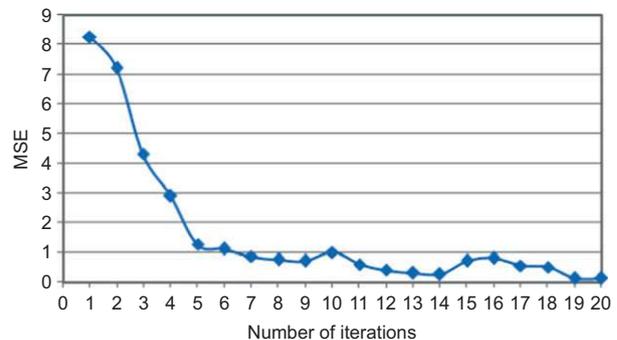

Figure 4 Number of iterations and the overall regression.

5.1 Neural network performance

From Table 2, although the overall regression is high (0.99048) for the network topology 3-16-3, the mean square error (MSE) is 8.6. However, for the architecture 3-20-3, the overall regression is 0.98106, which is marginally lower than the maximum value, but the MSE is 0.11, and hence, this architecture is finally considered. The plots between the number of iterations and the overall regression are shown in Figure 4. The MSE obtained for different iterations has been recorded and a plot for number of epochs and MSE for the topology is shown in Figure 5. It is evident that the value of MSE gradually decreases during the progress of training. An error of 8.6 initially is reduced to 0.11 after 20 iterations, and not much change has been found with further increase in the number of iterations.

5.2 Regression analysis

Data analysis includes test for significance of the regression model and test for significance on model coefficients, and ANOVA was performed. The designed experimental

Run	Topology	Regression analysis				MSE
		Training	Validation	Testing	Overall	
1	3-1-3	0.9451	0.99243	0.93757	0.94176	8.19
2	3-2-3	0.96898	0.95151	0.94709	0.96558	7.26
3	3-3-3	0.98108	0.98805	0.97557	0.97809	4.35
4	3-4-3	0.98686	0.98835	0.97546	0.97859	2.92
5	3-5-3	0.99237	0.9934	0.97478	0.97439	1.27
6	3-6-3	0.99319	0.97938	0.96299	0.98072	1.14
7	3-7-3	0.99592	0.98916	0.9494	0.98345	0.82
8	3-8-3	0.99704	0.99495	0.98373	0.98133	0.72
9	3-9-3	0.99681	0.96976	0.93108	0.98196	0.72
10	3-10-3	0.99774	0.94276	0.98946	0.97549	0.96
11	3-11-3	0.99778	0.97628	0.96576	0.96462	0.56
12	3-12-3	0.99841	0.96607	0.99419	0.98483	0.35
13	3-13-3	0.99894	0.92785	0.98797	0.98257	0.24
14	3-14-3	0.99878	0.96995	0.97603	0.97895	0.25
15	3-15-3	0.9976	0.94919	0.97284	0.96715	0.74
16	**3-16-3**	**0.99672**	**0.96604**	**0.90578**	**0.99048**	**0.86**
17	3-17-3	0.99312	0.92741	0.99762	0.96687	0.57
18	3-18-3	0.99463	0.93931	0.90504	0.97432	0.47
19	3-19-3	0.99931	0.94446	0.95749	0.97995	0.12
20	**3-20-3**	**0.99525**	**0.97994**	**0.9573**	**0.98106**	**0.11**

Table 2 Regression values and MSE calculated based on different network topologies.

Figure 5 Variation of the MSE of the trained data as a function of epochs (3-20-3).

Run	Thickness (mm)	Mass (N)	Height of fall (m)	Retardation at maximum load (m/s²)	Penetration at maximum load (mm)	Energy at maximum load (J)
1	2	35.32	0.5	571.44	4.889	14.584
2	4	35.32	1	1231.44	7.758	31.87
3	4	25.505	1	1604.998	9.302	25.173
4	4	15.69	1	2209.252	15.002	15.547
5	2	35.32	1.5	1219.429	18.246	28.564
6	6	15.69	1.5	2802.69	4.050	23.38
7	2	25.505	1	856.264	14.258	20.428
8	6	35.32	0.5	1240.19	5.021	17.381
9	4	25.505	1	1604.998	9.302	25.173
10	4	25.505	1	1604.998	9.302	25.173
11	6	15.69	0.5	1812.69	5.906	7.763
12	4	25.505	1.5	1643.075	5.355	30.32
13	4	25.505	1	1604.998	9.302	25.173
14	4	25.505	0.5	1295.19	12.543	12.537
15	6	25.505	1	1720.959	2.925	25.211
16	6	35.32	1.5	1240.19	1.25	48.226
17	4	25.505	1	1604.998	9.302	25.173
18	2	15.69	0.5	1129.252	15.596	7.696
19	2	15.69	1.5	1250.19	26.915	22.275
20	4	25.505	1	1604.998	9.302	25.173

Table 3 ANOVA table.

layout is shown in Table 3. To obtain accurate results, each combination of factors was repeated three times.

5.3 Checking the adequacy of the developed model

The fit summary recommended that the quadratic model is statistically significant for the analysis of retardation at the maximum load. The results of the quadratic model for retardation in the form of ANOVA are given in Table 4.
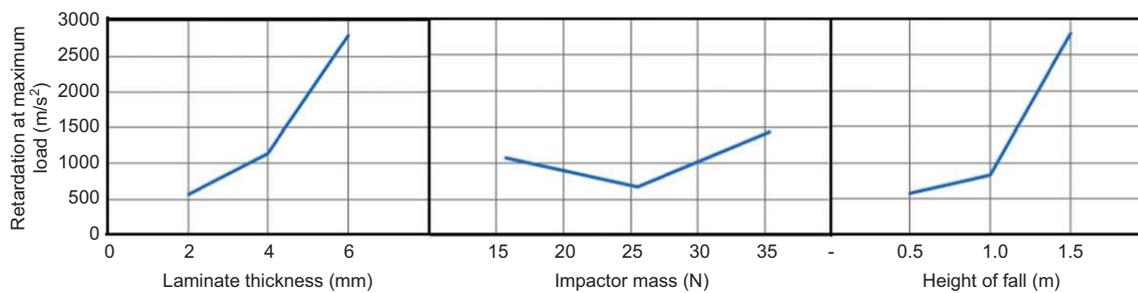
The value of R^2 was 91.93%. This means that regression model provides an excellent explanation of the relationship between the independent factors and the response. The associated p-value for the model is <0.05 (i.e., α=0.05, or 95% confidence interval), indicating that the model is considered statistically significant. Further, factors A, B, C, AB, and the second-order term of factor A have significant effect. The result shows that thickness

Source	Sum of squares	df	Mean square	F-value	p-Value (p>F)	Effect
Model	3.894E+006	9	3.894E+006	12.65	0.0002	Significant
Thickness (A)	1.437E+006	1	1.437E+006	42.00	<0.0001	Significant
Mass (B)	1.370E+006	1	1.370E+006	40.06	<0.0001	Significant
Height of fall (C)	4.439E+005	1	4.439E+005	12.98	0.0048	Significant
AB	2.989E+005	1	2.989E+005	8.74	0.0144	Significant
AC	6109.16	1	6109.16	0.18	0.6815	Insignificant
BC	26,790.22	1	26,790.22	0.78	0.3969	Insignificant
A^2	1.937E+005	1	1.937E+005	5.66	0.0386	Significant
B^2	76,068.74	1	76,068.74	2.22	0.1667	Insignificant
C^2	19,820.37	1	19,820.37	0.58	0.4641	Insignificant
Residual	3.420E+005	10	34,200.30			
Lack of fit	3.420E+005	5	68,400.61			
Pure error	0.000	5	0.000			
Cor. total	4.236E+006	19				

Table 4 ANOVA for response 1: retardation at maximum load (before elimination).
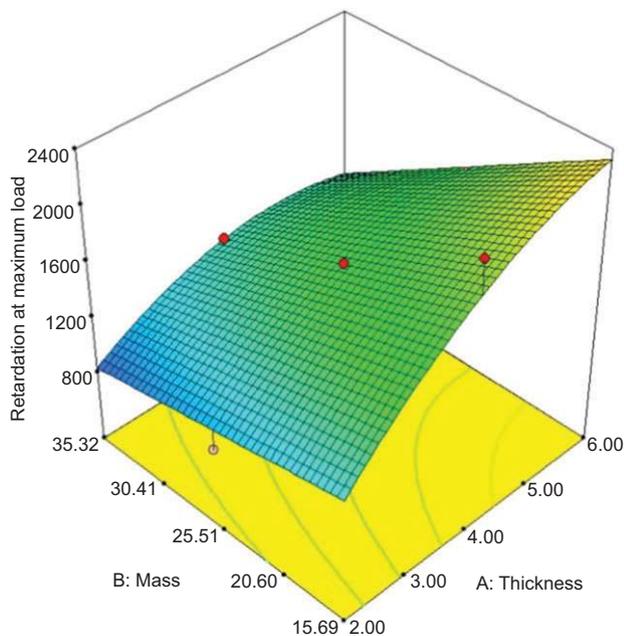R^2=0.9193, adjusted R^2=0.8466.

Source	Sum of squares	df	Mean square	F-value	p-Value (p>F)	Effect
Model	3.784E+006	5	7.568E+005	23.41	<0.0001	Significant
Thickness (A)	1.437E+006	1	1.437E+006	44.44	<0.0001	Significant
Mass (B)	1.370E+006	1	1.370E+006	42.38	<0.0001	Significant
Height of fall (C)	4.439E+005	1	4.439E+005	13.73	0.0024	Significant
AB	2.989E+005	1	2.989E+005	9.25	0.0088	Significant
A^2	2.345E+005	1	2.345E+005	7.25	0.0175	Significant
Residual	4.526E+005	14	32,328.22			
Lack of fit	4.526E+005	9	50,288.35			
Pure error	0.000	5	0.000			
Cor. total	4.236E+006	19				

Table 5 ANOVA for response 1: retardation at maximum load (after backward elimination). R^2=0.8932, adjusted R^2=0.8550.

Figure 6 Illustration of factor effects on retardation.

and mass are the most significant parameters for retardation at maximum load when compared with the height of fall because of higher F-value. The other model terms are said to be insignificant.

Figure 7 Effect of impactor mass and thickness on retardation.

The adequacy of the model was checked using ANOVA. Based on this technique, if the calculated value of the F-ratio of the developed model does not exceed the standard tabulated value of F-ratio for a desired level of confidence (say 99%), then the model is considered to be adequate within the confidence limit. The variance ratio, denoted by F in the ANOVA tables, is the ratio of the mean square due to a factor and the error mean square. In a robust design, the F-ratio can be used for qualitative understanding of the relative factor effects. A high F-value means that the effect of that factor is large compared with the error variance. Thus, the larger the value of F, the more important is that factor in influencing the process response.

To fit appropriately the quadratic model for retardation, the insignificant terms are eliminated by backward elimination. The ANOVA table for the reduced quadratic model for retardation at maximum load is shown in Table 5.

The reduced model results indicate that the model is significant (R^2 and adjusted R^2 are 89.32% and 85.50%, respectively). The significant effects based on F-values, in descending order, are factor A (thickness), factor B (impactor mass), factor C (height of fall), AB, and the second-order term of factor A (thickness). It can be seen that the regression model is fairly well fitted with the observed

Source	Sum of squares	df	Mean square	F-value	p-Value (p>F)	Effect
Model	633.07	9	70.34	11.65	0.0003	Significant
Thickness (A)	369.34	1	369.34	61.15	<0.0001	Significant
Mass (B)	91.97	1	91.97	15.23	0.0030	Significant
Height of fall (C)	14.12	1	14.12	2.34	0.1573	
AB	30.69	1	30.69	5.08	0.0478	Significant
AC	114.62	1	114.62	18.98	0.0014	Significant
BC	2.592E-003	1	2.592E-003	4.291E-004	0.9839	Insignificant
A^2	1.51	1	1.51	0.25	0.6277	Insignificant
B^2	11.52	1	11.52	1.91	0.1973	Insignificant
C^2	0.41	1	0.41	0.067	0.8009	Insignificant
Residual	60.40	10	6.04			
Lack of fit	60.40	5	12.08			
Pure error	0.000	5	0.000			
Cor. total	693.47	19				

Table 6 ANOVA for response 2: penetration at maximum load (before elimination).
$R^2=0.9129$, adjusted $R^2=0.8345$.

Source	Sum of squares	df	Mean square	F-value	p-Value (p>F)	Effect
Model	1527.66	9	169.74	37.13	<0.0001	Significant
Thickness (A)	80.74	1	80.74	17.66	0.0018	Significant
Mass (B)	409.14	1	409.14	89.50	<0.0001	Significant
Height of fall (C)	861.26	1	861.26	188.41	<0.0001	Significant
AB	56.64	1	56.61	12.39	0.0055	Significant
AC	40.06	1	40.06	8.76	0.0143	Significant
BC	26.75	1	26.75	5.85	0.0361	Significant
A^2	2.95	1	2.95	0.65	0.4403	Insignificant
B^2	0.059	1	0.059	0.013	0.9115	Insignificant
C^2	16.20	1	16.20	3.54	0.0892	Insignificant
Residual	45.71	10	4.57			
Lack of fit	45.71	5	9.14			
Pure error	0.000	5	0.000			
Cor. total	1573.37	19				

Table 7 ANOVA for response 3: energy at maximum load (before elimination).
$R^2=0.9709$, adjusted $R^2=0.9448$.

Source	Sum of squares	df	Mean square	F-value	p-Value (p>F)	Effect
Model	620.74	5	124.15	23.90	<0.0001	Significant
Thickness (A)	369.34	1	369.34	71.10	<0.0001	Significant
Mass (B)	91.97	1	91.97	17.70	0.0009	Significant
Height of fall (C)	14.12	1	14.12	2.72	0.1215	
AB	30.69	1	30.69	5.91	0.0291	Significant
AC	114.62	1	114.62	22.07	0.0003	Significant
Residual	72.73	14	5.19			
Lack of fit	72.73	9	8.08			
Pure error	0.000	5	0.000			
Cor. total	693.47	19				

Table 8 ANOVA for response 2: penetration at maximum load (after backward elimination).
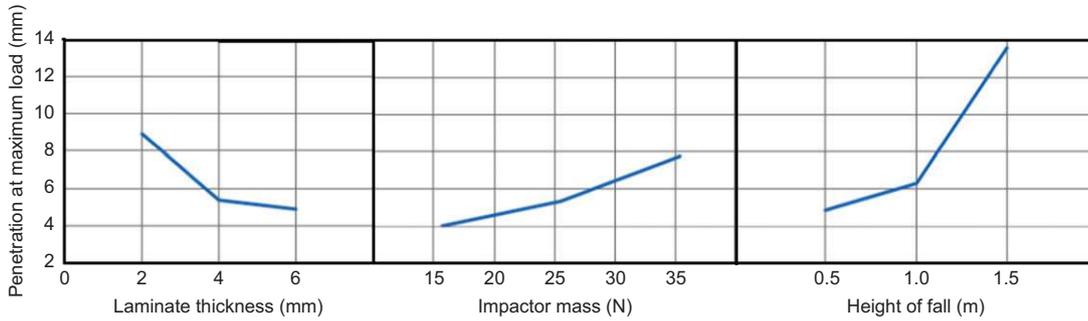$R^2=0.8951$, adjusted $R^2=0.8577$.

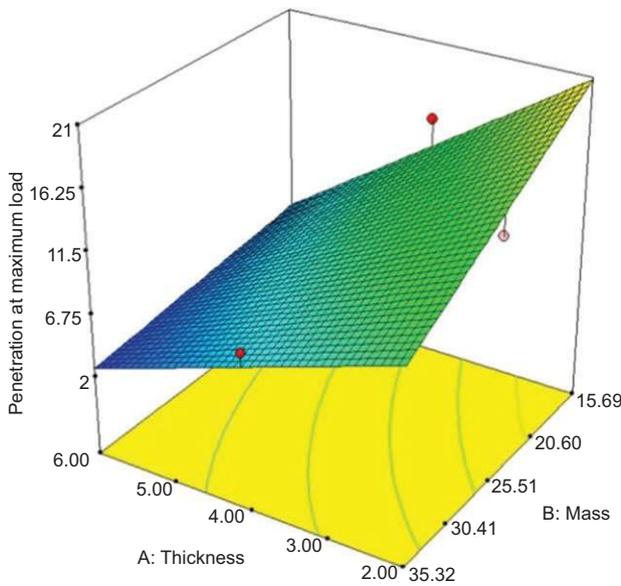**Figure 8** Illustration of factor effects on penetration.

Figure 9 Effect of impactor mass and thickness on penetration.

values. After eliminating the insignificant terms, the final response equation for retardation at maximum load is given in the following:

$$\text{Retardation at maximum load} = 1600.89 + 379.01$$
$$\times A{-}370.14 \times B + 210.68 \times C{-}193.30 \times A \times B{-}265.42 \times A^2 \quad (20)$$

The main factors influencing retardation are plotted in Figure 6. This plot is used to visualize the relation between the factors with the output response. There is a rapid increase in the retardation with an increase in the height of fall and thickness when compared with the effect of impactor mass. It is also evident that there is not much change in the retardation, whereas the impactor mass is increased from 15 to 30 N. The thickness of the laminates plays a vital role in increasing the retardation energy.

Figure 7 shows the estimated response surface for the retardation at maximum load in relation to the individual parameters of the impactor mass and laminate thickness. As can be seen from this figure, the retardation tends to increase slightly with an increase in impactor mass and increase steadily with an increase in laminate thickness. Because laminate thickness contributes to a higher level of bonding of layers, the rate of velocity decreases with an increase in thickness.

Similarly, the quadratic model for penetration and absorbed energy was developed. The results of the quadratic model for penetration and absorbed energy in the form of ANOVA are given in Tables 6 and 7.

To fit appropriately the quadratic model for penetration, the non-significant terms are eliminated by backward elimination. The ANOVA table for the reduced quadratic

Source	Sum of squares	df	Mean square	F-value	p-Value (p>F)	Effect
Model	1407.78	4	351.94	31.88	<0.0001	Significant
Thickness (A)	80.74	1	80.74	7.31	0.0163	Significant
Mass (B)	409.14	1	409.14	37.06	<0.0001	Significant
Height of fall (C)	861.26	1	861.26	78.01	<0.0001	Significant
AB	56.64	1	56.64	5.13	0.0387	Significant
Residual	165.60	15	11.04			
Lack of fit	165.60	10	16.56			
Pure error	0.000	5	0.000			
Cor. total	1573.37	19				

Table 9 ANOVA for response 3: energy at maximum load (after backward elimination).
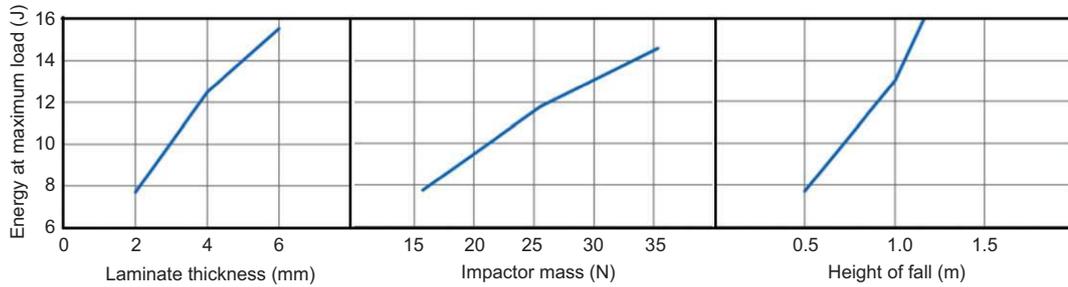$R^2 = 0.8948$, adjusted $R^2 = 0.8667$.

Figure 10 Illustration of factor effects on absorbed energy.

model for penetration at maximum load is shown in Table 8. The equation in terms of coded factors after backward elimination is

Penetration at maximum load=9.78-6.08
$$\times A\text{-}3.03\times B+1.19\times C+1.96\times A\times B\text{-}3.79\times A\times C \tag{21}$$

The factors influencing penetration at maximum load is plotted in Figure 8. This plot is used to visualize the relation between the factors with the output response. There is a rapid increase in penetration only when there is an increase in the height of fall. The other two factors show resistance to penetration. Figure 9 shows the estimated response surface for the penetration in relation to the individual parameters of the thickness of the laminate and the impactor mass. As can be seen from this figure, the penetration tends to increase steadily with an increase in impactor mass and tends to decrease with an increase in the thickness of the laminates because the thickness of the laminates contributes to the rebounding of the dart.

To fit appropriately the quadratic model for absorbed energy, the non-significant terms were eliminated by backward elimination. The ANOVA table for the reduced quadratic model for energy at maximum load is shown in Table 9.

The reduced model results indicate that the model is significant (R^2 and adjusted R^2 are 89.48% and 86.67%, respectively). The significant effects based on F-values, in descending order, are factor C, factor B, factor A, and factor AB.

It can be seen that the regression model is fairly well fitted with the observed values. The equation in terms of coded factors after backward elimination is

Energy at maximum load=22.84+2.84$\times A$+6.40$\times B$+9.28
$$\times C+2.66\times A\times B \tag{22}$$

The factors influencing energy at maximum load is plotted in Figure 10. There is a rapid increase in energy at maximum load with an increase in height of fall when compared with the other two factors. It is also evident
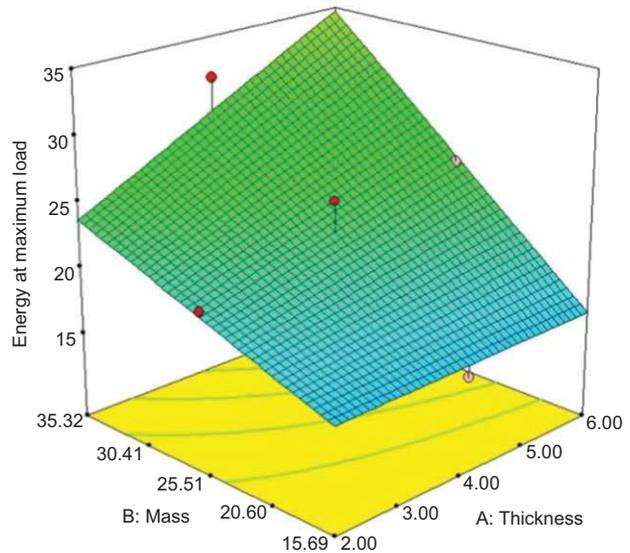

Figure 11 Effect of impactor mass and thickness on energy at maximum load.

that there is a slight change in the absorbed energy when the impactor mass is increased. Figure 11 shows the estimated response surface for the absorbed energy at maximum load in relation to the individual parameters of laminate thickness and impactor mass. As can be seen from this figure, the energy tends to increase steadily with an increase in impactor mass and no significant change with an increase in laminate thickness. Because the impactor mass contributes to the increase in velocity, the absorbed energy increases with an increase in the impactor mass.

6 Conclusions

A new methodology based on ANNs has been developed to study the low-velocity impact characteristics on woven glass epoxy laminates of EP3 grade. The following conclusions are drawn from the results of the BPNN model

and statistical analysis. Based upon the correlation coefficient, error distribution, and convergence, different BPNN architectures are trained/analyzed using the experimental data until an optimum architecture was identified. Among them, the BPNN with one hidden layer having 20 neurons trained with Levenberg-Marquardt algorithm was found to be the optimum network model (3-20-3). An error of 8.6 initially is reduced to 0.11 after 20 iterations, and not much change has been found with further increase in the number of iterations. A sound performance was achieved with the neural network model, with good correlation coefficient (between predicted and experimental values), high uniform error distribution, and the convergence of the entire data set within the permissible error range.

From the empirical modeling and with help of RSM, it was observed that the retardation tends to increase slightly with an increase in impactor mass and steadily increase with an increase in laminate thickness. It was seen that the height of the fall of the impactor has been less significant on retardation when compared with laminate thickness. Penetration tends to increase steadily with an increase in impactor mass and decreases with an increase in laminate thickness. There is a rapid increase in energy at maximum load with an increase in impactor mass when compared with the other two factors. It is also evident that there is a slight change in the absorbed energy when the thickness is increased. Finally, the developed mathematical model successfully predicted the output parameters of laminates subjected to low-velocity impact.

References

[1] Abrate S. *Appl. Mech. Rev.* 1991, 44, 155–189.
[2] Cantwell WJ, Morton J. *Compos. Part A Appl. S.* 1991, 22, 347–362.
[3] Richardson MOW, Wisheart MJ. *Compos. Part A Appl. S.* 1996, 27, 1123–1131.
[4] Rajesh Mathivanan N, Jerald J. *Mater. Des.* 2010, 31, 4553–4560.
[5] Davies GAO, Hitchings D, Zhou G. *Compos. Part A Appl. S.* 1996, 27A, 1147–1156.
[6] Lifshitz JM, Gandelsman M. *Compos. Sci. Technol.* 1997, 57, 205–216.
[7] Ebeling T, Hiltner A. *J. Compos. Mater.* 1997, 31, 1318–1333.
[8] Hirai Y, Hamada H, Kim JK. *Compos. Sci. Technol.* 1998, 58, 91–104.
[9] Wu E, Chang LC. *J. Compos. Mater.* 1998, 32, 702–721.
[10] El Kadi H. *Compos. Struct.* 2006, 73, 1–23.
[11] Chandrashekhara K, Okafor A, Jiang Y. *Compos. Part B Eng.* 1998, 29, 363–370.
[12] Bezerra EM, Ancelotti AC, Pardini LC, Rocco JAFF, Iha K, Ribeiro CHC. *Mater. Sci. Eng. A.* 2007, 464, 177–185.
[13] Chakraborty D. *Mater. Des.* 2005, 26, 1–7.
[14] Graham D, Maas P, Donaldson GB, Carr C. *NDT&E Int.* 2004, 37, 565–570.
[15] Fernández-Fdz J, López-Puente R, Zaera A. *Compos. Part A Appl. S.* 2008, 39, 989–996.
[16] Myers RH, Montgomery DC. *Response Surface Methodology*, John Wiley & Sons: New York, 2002.
[17] Derringer G, Suich R. *J. Qual. Technol.* 1980, 12, 214–219.
[18] George PM, Raghunath BK, Manocha LM, Warrier AM. *J. Mater. Process. Technol.* 2004, 153–154, 920–924.
[19] Kansal HK, Singh S, Kumar P. *J. Mater. Process. Technol.* 2005, 169, 427–436.
[20] ASTM D3029, *Standard Test Method for Impact Resistance of Rigid Plastic Sheeting or Parts by Means of a Tup (Falling Weight)*, American Society for Testing and Materials: Philadelphia, PA, 1982.
[21] Tiago C, Leitão V. *Compos. Math. Appl.* 2006, 51, 1311–1314.
[22] Deng J. *Int. J. Solid Struct.* 2006, 43, 3255–3291.
[23] Príncipe JC, Neil RE, Lefebvre C. *Neural and Adaptive Systems: Fundamentals Through Simulations*, John Wiley & Sons: New Jersey, USA, 1999.
[24] Hosseini M, Abbas H. *Thin-Walled Struct.* 2008, 46, 592–601.
[25] Malinov S, Sha W, McKeown JJ. *Comput. Mater. Sci.* 2001, 21, 375–394.
[26] Fausett L. *Fundamentals of Neural Networks Architectures, Algorithms and Applications*, Pearson Education: India, 2004.